

Efficiency Enhancement of GaAs Thermophotovoltaic Cells System using Integrated $\text{TiO}_2/\text{SiO}_2$ 1D Photonic Crystal Distributed Bragg Reflectors

Praveen Kumar Yadav,^{*1} Rishi Pal Chahal,² and Aman Pal Singh¹

¹*Department of Physics, University of Rajasthan, Jaipur, Rajasthan, India-302004*

²*Department of Physics, Choudhary Bansi Lal University, Bhiwani, Haryana, India-127021*

Received September 24, 2025; accepted December 22, 2025; published December 31, 2025

Abstract—Thermophotovoltaic (TPV) systems rely on spectrally selective reflectors to enhance conversion efficiency by maximizing photon flux above the photovoltaic bandgap while suppressing sub-bandgap thermal losses. This work presents a numerical analysis and simulation of $\text{SiO}_2/\text{TiO}_2$ multilayer photonic crystal Distributed Bragg Reflectors (DBRs) tailored to the GaAs bandgap (≈ 872 nm). The Transfer Matrix Method (TMM) was applied to investigate the optical properties of the structure, taking into account the layer's thickness, number of periods, and refractive index contrast. Investigation demonstrates that an optimized multilayer design exhibits narrowband reflection peaks centered around 800–1000 nm (\approx approximately 200 nm), closely matching the GaAs photovoltaic cutoff wavelength, with reflectivity exceeding 0.99. Beyond 1000 nm, reflectivity is strongly suppressed, minimizing energy reflections associated with unusable infrared photons. The stability analysis, considering both angular and polarization effects, suggests robust performance over a wide range of angles of incidence, which is a critical requirement for practical and efficient TPV operations. The numerical and simulation findings highlight the potential of $\text{SiO}_2/\text{TiO}_2$ 1D photonic crystal thermally stable, tunable selective reflectors, offering a viable pathway for efficiency enhancement in GaAs-based TPV systems.

The energy conversion through thermophotovoltaic (TPV) systems has emerged as a promising approach for directly generating electricity from heat, with potential applications in waste heat recovery, concentrated solar power, and compact power supplies for aerospace and defense. The limitations of conventional TPV systems lie in the mismatch between the broadband emission of thermal sources and the narrow spectral response of thermophotovoltaic (TPV) cells. A large amount of the emitted radiation falls outside the useful band of the TPV cells, resulting in significant efficiency losses. Using selective reflector structures tailored to match the PV cell band gaps for thermal radiation is an effective strategy to address this challenge. Therefore, enhancing photon reflections in the desired spectral range while suppressing/passing long-wavelength losses. Thus, selective reflectors can substantially improve TPV conversion efficiency [1–3].

Various material platforms have been explored for selective thermal reflections, including refractory metals, plasmonic meta-surfaces, and dielectric multilayers. Among these, one-dimensional (1D) photonic crystals composed of alternating dielectric films are particularly interesting. These 1D PhC combine sharp spectral selectivity with high reflectivity control and remain stable under high-temperature operation. A multilayered stack of $\text{SiO}_2/\text{TiO}_2$ 1D PhCs has drawn significant attention due to its high refractive index contrast, low absorption losses in the near-infrared region (NIR), and fabrication using conventional thin-film deposition techniques [4–6]. Studies in this field have confirmed their robustness at elevated temperatures. Further, $\text{SiO}_2/\text{TiO}_2$ nano multilayers maintain high reflectivity ($\approx 75\%$) across 600–1600 nm even at 1350 °C [7]. Inorganic $\text{SiO}_2/\text{TiO}_2$ meta-materials can be engineered to control reflectivity [8, 9]. Spectrum-tailorable reflectors based on silicon and titanium dielectric stacks have been proposed, underscoring their precise control of reflection peaks while ensuring high-temperature stability [10].

The optical properties and design of these 1D PhC multilayers have been widely studied using numerical methods, including the transfer matrix method (TMM), to investigate how the number of $\text{SiO}_2/\text{TiO}_2$ periods, layer thicknesses, and incidence angles affect photonic crystal filtering for TPV applications [11]. Zhou, Yehia, and Bermel designed chirped $\text{SiO}_2/\text{TiO}_2$ quarter-wave stacks integrated into selective emitters, demonstrating strong suppression of unwanted sub-band gap emission [12]. These works illustrate both the methodological maturity and the strong application potential of $\text{SiO}_2/\text{TiO}_2$ systems in TPV technology.

* E-mail: praveenuor3@gmail.com



© 2025 by the (authors list). This article is an open access article distributed under the terms and conditions of the Creative Commons Attribution (CC BY) license (<https://creativecommons.org/licenses/by/4.0/>).

In this work, a comprehensive numerical study of $\text{SiO}_2/\text{TiO}_2$ multilayer 1D photonic crystal reflectors designed for GaAs-based TPV systems has been conducted. By applying the transfer matrix method, the spectral reflectivity of these structures across different geometrical configurations is analyzed, and their angular and polarization dependence are examined. The results show that carefully engineered multilayer stacks can achieve narrow, high-reflectivity peaks tuned to the GaAs band gap ($\approx 872 \text{ nm}$), while suppressing/passing unwanted long-wavelength emissions [13]. These findings demonstrate the promise of dielectric multilayer reflectors as practical, thermally stable solutions for TPV applications, providing a foundation for further optimization and experimental validation.

The performance of the thermophotovoltaic (TPV) cell system depends critically on the spectral matching between the thermal emitter and the TPV cell. For a GaAs cell with a direct bandgap of $E_g \approx 1.42 \text{ eV}$ ($\lambda_g \approx 872 \text{ nm}$), the photons whose energy is below the bandgap cannot generate an electron-hole pair and are lost as heat [14]. An efficient emitter must therefore maximize emissivity in the near-infrared band just above the GaAs band gap, while suppressing long-wavelength emission to minimize radiative losses.

Photonic crystals, consisting of periodic dielectric stacks, enable spectral tailoring of thermal emission through constructive and destructive interference of optical modes. The photonic band gaps form the forbidden frequency ranges for the propagation [15-17]. For a quarter-wave Bragg's stack composed of alternating materials with refractive indices η_H and η_L and thicknesses d_H and d_L , the central stopband wavelength is given by the equation:

$$\lambda_0 = 2(\eta_H d_H + \eta_L d_L). \quad (1)$$

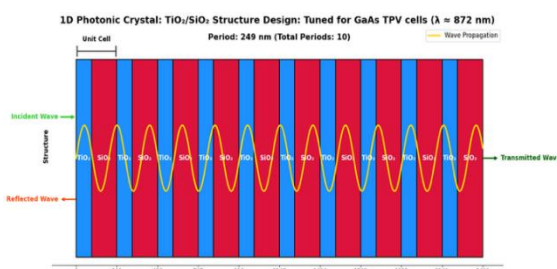


Fig. 1. One-dimensional Photonic Crystal DBR structure tuned for GaAs TPV Cell: Periodic stack of alternating $\text{TiO}_2/\text{SiO}_2$ layers, where: $d_1 = 94 \text{ nm}$, $d_2 = 155 \text{ nm}$, and $d = d_1 + d_2 = 249 \text{ nm}$ for $N = 10$.

By choosing materials with a significant refractive index contrast, as in this study TiO_2 ($n \approx 2.4$) and SiO_2 ($n \approx 1.45$) are taken. In the near-infrared region (NIR), strong reflection bands can be achieved with relatively few periods and varying thicknesses.

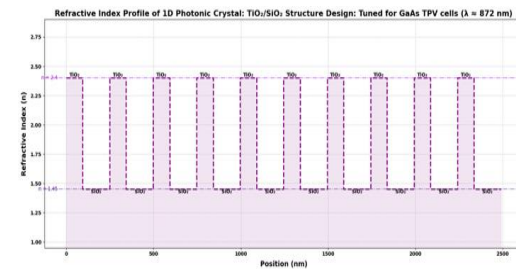


Fig. 2. Refractive index profile of one-dimensional Photonic Crystal DBR structure tuned for GaAs TPV Cell: Periodic stack of alternating $\text{TiO}_2/\text{SiO}_2$ layers, where $d_1 = 94 \text{ nm}$, $d_2 = 155 \text{ nm}$, and $d = d_1 + d_2 = 249 \text{ nm}$ for $N = 10$.

Thermal reflections from such a multilayer structure can then be derived from Kirchhoff's law, according to which emissivity $\epsilon(\lambda, \theta)$ equals absorptivity $\alpha(\lambda, \theta)$ under thermal equilibrium. Since absorption is related to transmittance T and reflectance R as given by the following equation:

$$\alpha(\lambda, \theta) = 1 - R(\lambda, \theta) - T(\lambda, \theta). \quad (2)$$

The absorptance spectrum of the multilayer stack can be obtained from optical simulations of R and T . The Transfer Matrix Method (TMM) is employed for modeling wave propagation in stratified media. Each dielectric layer j of thickness d_j and refractive index η_j contributes a propagation matrix as given by equation [18]:

$$M_j = \begin{bmatrix} \cos(\phi_j) & \cdots & \frac{i}{q_j} \cdot \sin(\phi_j) \\ \vdots & \ddots & \vdots \\ i q_j \sin(\phi_j) & \cdots & \cos(\phi_j) \end{bmatrix}, \quad (3)$$

where $\phi_j = \frac{2\pi}{\lambda} \eta_j d_j \cos \theta_j$ is the phase accumulated in the layer, and q_j depends on the polarization (TE or TM). For TE polarization,

$$q_j = \frac{\eta_j \cdot \cos \theta_j}{\eta_0 \cdot \cos \theta_0}, \quad (4)$$

while for TM polarization,

$$q_j = \frac{\eta_0 \cdot \cos \theta_0}{\eta_j \cdot \cos \theta_j}. \quad (5)$$

To find out the transfer matrix for the whole system, multiply the matrices of each layer in order:

$$M = \prod_{j=1}^N M_j. \quad (6)$$

Using TMM transmission as well as reflection coefficients had been derived, which are given by equations:

$$R = |r|^2, \quad (7)$$

$$T = |t|^2 \cdot \frac{\eta_s \cdot \cos \theta_s}{\eta_0 \cdot \cos \theta_0}, \quad (8)$$

where η_0 and η_s are the refractive indices of the incident and substrate media, respectively. Finally, the emissivity is obtained from the equation:

$$\epsilon(\lambda, \theta) = 1 - R(\lambda, \theta) - T(\lambda, \theta). \quad (9)$$

Figures 3, 4, and 5 show the results of the simulation and numerical analysis. $\text{TiO}_2/\text{SiO}_2$ 1D (one-dimensional) photonic crystal DBRs are a powerful tool for managing the spectrum in GaAs-based TPV cell systems. In Fig. 4, it is shown that by reflecting low-energy ($\lambda \approx 950-1400$ nm) photons back toward the thermal emitter, the DBRs promote photon recycling, giving those photons another chance to be re-emitted at higher energies that the GaAs cell system can absorb. Furthermore, Fig. 3 illustrates that it can be designed to match the back reflection of photons ($\lambda \approx 800-1050$ nm), which aligns with the band gap of the GaAs TPV cell system. This will provide another opportunity for the TPV to absorb the matching photons.

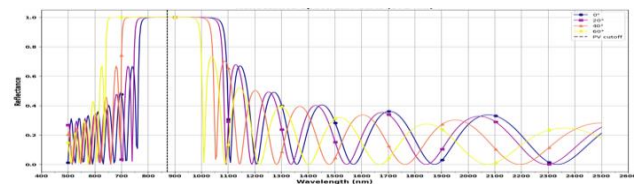


Fig. 3. Reflectance Spectrum of $\text{TiO}_2/\text{SiO}_2$ one-dimensional (1D) Photonic Crystal DBR tuned for GaAs TPV cell, where $d_1 = 94$ nm, $d_2 = 155$ nm, and $d = d_1 + d_2 = 249$ nm for $N = 10$.

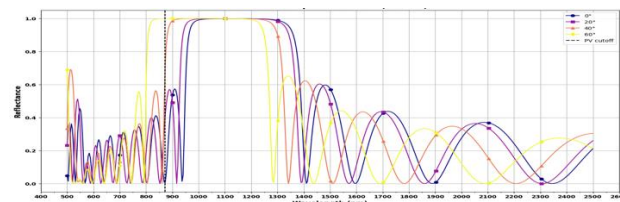


Fig. 4. Reflectance Spectrum of $\text{TiO}_2/\text{SiO}_2$ one-dimensional (1D) Photonic Crystal DBR tuned for GaAs TPV cell, where $d_1 = 120$ nm, $d_2 = 190$ nm, and $d = d_1 + d_2 = 310$ nm for $N = 8$.

This design achieves a wide stopband with only a modest number of bilayers, striking a practical balance between strong optical performance and manageable fabrication requirements. There is an angular dependence of stop bands, which can lead to reduced reflectivity compared to normal incidence. This angular dependence indicates a blue shift (a shift towards shorter wavelengths) with an increase in angle of incidence, as illustrated in Figs. 3 and 4. This shift is approximately 110 nm, from normal to a 60° angle of incidence. Overall, integrating $\text{TiO}_2/\text{SiO}_2$ DBRs with GaAs TPV cells provides effective spectral control, reduces parasitic losses, and delivers a measurable efficiency boost. These findings highlight DBR-assisted designs as a promising pathway toward the next generation of high-performance thermophotovoltaic technologies.

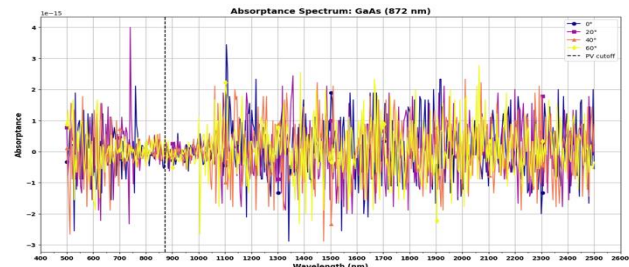


Fig. 5. Absorptance Spectrum of $\text{TiO}_2/\text{SiO}_2$ one-dimensional (1D) Photonic Crystal DBR tuned for GaAs TPV cell, where $d_1 = 94$ nm, $d_2 = 155$ nm, and $d = d_1 + d_2 = 249$ nm for $N = 10$.

References

- [1] Z. Omair, S. Hooten, V. Menon, P. Oduor, K.-K. Choi, A.K. Dutta, Opt. Express **32**, 11000 (2024).
- [2] A. LaPotin, K.L. Schulte, M.A. Steiner *et al.* Nature **604**, 287 (2022); <https://doi.org/10.1038/s41586-022-04473-y>.
- [3] T. Inoue, T. Suzuki, K. Ikeda, T. Asano, S. Noda, Opt. Express **29**, 11133 (2021).
- [4] J. Choi, K. Han, J.H. Kim, Thin Solid Films **569**, 100 (2014); doi: <https://doi.org/10.1016/j.tsf.2014.08.036>.
- [5] A. Kotbi, W.E. Hakim, P. Barroy *et al.*, Opt. Quant. Electron. **57**, 534 (2025); <https://doi.org/10.1007/s11082-025-08455-y>.
- [6] J. Xi, E. Schubert, D. Ye, T. Lu, S.H. Lin, J. Juneja, Opt. Lett. **31**, 601 (2026); doi: <https://doi.org/10.1364/OL.31.000601>.
- [7] G. Christidis, O. Fabrichnaya, S. Koepfli, E. Poloni, J. Winiger, Y. Fedoryshyn, A. Gusarov, M. Ilatovskaya, I. Saenko, G. Savinykh, V. Shklover, J. Leuthold, J. Materials Science **56**, 18440 (2021); doi: <https://doi.org/10.1007/s10853-021-06557-y>.
- [8] D. Kim, K.M. Kim, H. Han *et al.*, Sci Reports **12**, 32 (2022); doi: <https://doi.org/10.1038/s41598-021-03935-z>
- [9] G. Hwang, G. Bak, Y. Kim, S.H. Jung, H. Na, Y.J. Jung, ACS Omega **10**(32), 36582 (2025); doi: <https://doi.org/10.1021/acsomega.5c05459>.
- [10] S. Chen, T. Zhu, F. Juan, Y. Zhu, J. Xu, K. Chen, Solar Energy **276**, 112664 (2024); <https://doi.org/10.1016/j.solener.2024.112664>.
- [11] F.K. Mbakop, R.Z. Falama, F. Wu, A. Ayang, S.N. Essiane, L. Leontie, N. Djongyong, F. Iacomi, Results in Optics **14**, 100594 (2024); <https://doi.org/10.1016/j.rio.2023.100594>.
- [12] Z. Zhou, O. Yehia, P. Bermel, J. Nanophoton. **10**(1) 016014 (2016); <https://doi.org/10.1117/1.JNP.10.016014>.
- [13] M.B. Panish, H.C. Casey, J. Appl. Phys. **40**(1), 163 (1969); doi: <https://doi.org/10.1063/1.1657024>.
- [14] M. Suemitsu, T. Asano, T. Inoue, S. Noda, ACS Photonics **7**(1), 80 (2020); doi: [10.1021/acspophotonics.9b00984](https://doi.org/10.1021/acspophotonics.9b00984).
- [15] L. Farah, A.B. Hadjira, A. Mehadji, Photon. Lett. Poland **8**(3), 82 (2016).
- [16] N.L. Kazanskiy, M.A. Butt, Photon. Lett. Poland **12**(3), 85 (2020).
- [17] O.H. Jaworska, S. Ertman, Photon. Lett. Poland **9**(3), 79 (2017).
- [18] D.M. Mead, J. Sound Vibration **190**(3), 495 (1996).